

Ab-initio calculations for the β -tin diamond transition in Silicon: comparing theories with experiments

Sandro Sorella,^{1,2} Michele Casula,³ Leonardo Spanu,⁴ and Andrea Dal Corso^{1,2}

¹*International School for Advanced Studies (SISSA), Via Bonomea 265, 34136 Trieste, Italy*

²*DEMOCRITOS Simulation Center CNR-IOM Istituto Officina dei Materiali, 34151, Trieste, Italy*

³*CNRS and Institut de Minéralogie et de Physique des Milieux condensés,
case 115, 4 place Jussieu, 75252, Paris cedex 05, France*

⁴*Department of Chemistry, University of California at Davis, Davis, CA, USA*

(Dated: November 12, 2010)

We investigate the pressure-induced metal-insulator transition from diamond to β -tin in bulk Silicon, using quantum Monte Carlo (QMC) and density functional theory (DFT) approaches. We show that it is possible to efficiently describe many-body effects, using a variational wave function with an optimized Jastrow factor and a Slater determinant. Variational results are obtained with a small computational cost and are further improved by performing diffusion Monte Carlo calculations and an explicit optimization of molecular orbitals in the determinant. Finite temperature corrections and zero point motion effects are included by calculating phonon dispersions in both phases at the DFT level. Our results indicate that the theoretical QMC (DFT) transition pressure is significantly larger (smaller) than the accepted experimental value. We discuss the limitation of DFT approaches due to the choice of the exchange and correlation functionals and the difficulty to determine consistent pseudopotentials within the QMC framework, a limitation that may significantly affect the accuracy of the technique.

PACS numbers:

I. INTRODUCTION

The prediction of material behavior under pressure is of great relevance in several branches of science, ranging from material science to planetary physics¹. The experimental determination of pressure effects on the phase diagram can be rather complicated even for simple inorganic crystal, due to the related extreme conditions or the existence of subtle phenomena, such as hysteresis. In this respect, *ab-initio* calculations are complementary methods for determining phase diagrams and understanding material phases in a large range of pressures and temperatures.

The density functional theory (DFT) has been widely used for describing material behavior under pressure. However, when a transition is accompanied by a drastic change in the electronic structure, non-canceling errors in the two phases can lead to a significant bias in the predicted transition pressure. That is the case of bulk Silicon (Si), where the diamond-to- β -tin transition is associated with a semiconductor-to-semimetal electronic change. For this reason, the Si diamond-to- β -tin transition has been used for testing and benchmarking new *ab-initio* numerical approaches for extended systems. Its first order nature makes it a difficult case for the experiments²⁻⁴. The accepted experimental values for the transition pressure are in between 10 and 12.5 GPa at room temperature, the difference could be ascribed to non hydrostatic conditions⁵, non quenched metastable phases⁶, and presence of lattice defects⁷.

Theoretical calculations based on DFT strongly depend on the choice of exchange and correlation (XC) functional. Calculations based on the local density ap-

proximation (LDA) predict a zero temperature transition pressure p_t in the range of 7.2⁸-8.2⁹ GPa (this difference could be explained by the type of pseudopotential (PP) used). The generalized gradient approximation (GGA) leads to p_t in the range of 12.2¹⁰-13.5⁸ GPa with the Perdew-Wang functional¹¹. Moreover, in the case of the PBE functional¹², a value of 10.2 GPa is obtained in Ref. 9. Since the PBE functional fulfills a number of exact DFT properties, this should be considered the state-of-the-art among the most accurate *ab-initio* functionals. A careful investigation of the effect of the XC functional on the transition pressure was done recently in Ref. 13, where the authors show that the inclusion of non-local exchange in the XC functional leads to a significant improvement of the estimate of the transition pressure. All the calculations are performed at zero temperature and therefore a comparison with experiments is possible only after including zero-point motion and finite temperature effects. This accounts for a significant reduction of the transition pressure, as estimated in Ref.14 by means of the LDA functional, with a correction larger than 1GPa. Moreover the explicit inclusion of non linear core corrections (NLCC) in pseudopotential calculations further reduces the transition pressure.

Quantum Monte Carlo (QMC) methods can be an alternative to DFT-based approaches. In the past years, many authors have shown practical applications of QMC methods for computing the energetics of extended systems^{15,16}, and predicting crystal phases under pressure^{17,18}. In a early work, Alfé *et al.*¹⁸ used diffusion Monte Carlo (DMC) for investigating the Si diamond-to- β -tin transition. They calculated a QMC transition pressure of 16.5 GPa, namely 4-5 GPa larger than the ex-

perimental range. The discrepancy was attributed to the fixed-node (FN) approximation¹⁹, since the other source of errors (time step error, pseudopotential locality error, size effects) were considered negligible. More recently, Purwanto *et al.*²⁰ obtained a transition pressure of 12.6 using the auxiliary-field QMC (AFQMC) method with the phaseless approximation to cure the sign problem, whose bias has been shown to be very small²¹. The very recent DMC calculation in Ref. 13, carried out with the most advanced optimization²² and size-extrapolation²³ methods, gives a transition pressure of 14 GPa in substantial agreement with the AFQMC one, although the latest DMC value is affected by a larger uncertainty (1GPa).

In the present work, we address the problem of the Si diamond-to- β -tin zero temperature transition by performing variational Monte Carlo (VMC) calculations for the total energy of the two crystal structures. VMC is not affected by the sign problem and has proven to be a reliable approach for several systems^{15,16,24,25}. The accuracy of the method depends entirely on the choice of the variational wave function, and the capability of finding its optimal form. In this work, we show that with a relative simple parameterization of the wave function (WF) we are able to describe correlation effects across the metal-insulator transition. Our wave function is a product of a Jastrow factor and a Slater determinant. The variational optimization of the Jastrow factor has a relative small computational cost²², and it reveals an accurate way to build-up correlation effects starting from an LDA calculation.

The paper is organized as follows. In Sec. II we review the properties of our variational wave function, we present a systematic study of the basis set used for the calculations, and we discuss the correction of the finite size errors. In Sec. III we review sources of errors not directly estimated at the QMC level, such as the quantum and thermal lattice energies, and the accuracy of the PP's. This will help us to make a fair comparison between our results and the most significant experimental and theoretical findings reported in literature. In Sec. IV we report our results, while in Sec. V we draw our conclusions.

II. COMPUTATIONAL DETAILS

In our investigation we have carried out DFT calculations with the Quantum Espresso (QE)²⁶, Wien2K²⁷ and *Qbox*²⁸ packages, and we used the *TurboRVB* code²⁹ to perform variational Monte Carlo (VMC) and Lattice Regularized Diffusion Monte Carlo (LRDMC)³⁰ calculations. In both DFT and QMC the system is described by an effective Hamiltonian in the Born-Oppenheimer approximation (without quantum effects of lattice vibrations) with the core electrons treated neon-core PP.

For extensive volume (pressure) dependent calculations, we used the relativistic Hartree-Fock PP's gen-

erated by Trail and Needs³¹, employed also in previous QMC calculations of Refs. (13,18). To check the impact of the PP approximation we carried out single-volume calculations using the Burkatzki-Filippi-Dolg energy-adjusted PP's³² and the ones generated by the atomic PWSCF code²⁶ with the Troullier-Martins construction³³ from relativistic LDA and PBE atomic calculations. The PP's are expanded in a semilocal form in terms of Gaussians⁵⁶.

A. Wave function and localized basis set

Our many-body wave function is the product of a Slater determinant and a many-body Jastrow factor. Alternatively, in the case of open shell systems, we use the Jastrow-correlated Antisymmetrized Geminal Power (JAGP)²⁵.

The electron correlation is included in our wave function through the Jastrow factor $J(\mathbf{r}_1, \dots, \mathbf{r}_N) = \prod_{i < j} \exp(f(\mathbf{r}_i, \mathbf{r}_j))$, where $f(\mathbf{r}, \mathbf{r}')$ is assumed to depend only upon two-electron coordinates, and N is the total number of electrons. The function f is expanded in a basis of Gaussian atomic orbitals $\bar{\phi}_i$, such that it reads:

$$f(\mathbf{r}, \mathbf{r}') = \sum_{i,j} g_{ij} \bar{\phi}_i(\mathbf{r}) \bar{\phi}_j(\mathbf{r}'). \quad (1)$$

The convergence of this expansion is improved by adding an homogeneous term and a one-body contribution, thus satisfying the electron-electron and the electron-ion cusp conditions, respectively^{25,34}. The basis set used for the Jastrow includes $2s2p$ Gaussian orbitals.

For system with large number of electrons, we improve the efficiency of the optimization procedure and its computational cost, adopting an explicit parameterization of the Jastrow factor. Given two generic orbitals $\bar{\phi}_i$ and $\bar{\phi}_j$, the variational coefficient $g_{ij} = g_{ij}(\mathbf{R}_{ij})$ in Eq. 1 depends only on the orbital symmetry (in this case either s or p) and the distance vector \mathbf{R}_{ij} between the corresponding atomic centers. g_{ij} is optimized without constraint when the two orbitals are localized on the same atom (i.e. $\mathbf{R}_{ij} = 0$). Otherwise $g_{ij}(\mathbf{R}_{ij})$ is parameterized in a way to recover an isotropic large distance correlation. For the sake of clarity, we define \mathbf{p}_j as the vector containing the three x, y, z p-orbital components centered at a given atomic position \mathbf{R}_j , and with s_j we indicate the s-wave orbital located at the same position. By this notation we can write four possible isotropic invariant contributions

for $\mathbf{R}_{ij} \neq 0$, such that:

$$\begin{aligned} \sum_{\substack{l=s_i, \mathbf{p}_i \\ m=s_j, \mathbf{p}_j}} g_{lm} \bar{\phi}_l \bar{\phi}_m &= f_1(R_{ij}) \bar{\phi}_{s_i} \bar{\phi}_{s_j} \\ &+ f_2(R_{ij}) (\bar{\phi}_{s_i} \mathbf{r}_{ij} \cdot \bar{\phi}_{\mathbf{p}_j} + \mathbf{p} \leftrightarrow s) \\ &+ f_3(R_{ij}) (\mathbf{r}_{ij} \cdot \bar{\phi}_{\mathbf{p}_i}) (\mathbf{r}_{ij} \cdot \bar{\phi}_{\mathbf{p}_j}) \\ &+ f_4(R_{ij}) (\bar{\phi}_{\mathbf{p}_i} \cdot \bar{\phi}_{\mathbf{p}_j}) \end{aligned} \quad (2)$$

where $R_{ij} = |\mathbf{R}_{ij}|$, and $\mathbf{r}_{ij} = \mathbf{R}_{ij}/R_{ij}$ is the unit vector connecting the atomic centers i and j . The functions $f_p(R_{ij})$ are polynomials which read:

$$\begin{aligned} f_p(R_{ij}) &= C_0^p \log(R_{ij}) + \sum_{k=1}^{k=2} C_k^p R_{ij}^{-k} \quad \text{for } p = 1, 2 \\ f_p(R_{ij}) &= \sum_{k=1}^{k=3} C_k^p R_{ij}^{-k} \quad \text{for } p = 3, 4 \end{aligned} \quad (3)$$

The scalar functions in Eq. 3 depend only on 12 variational parameters, optimized via energy minimization³⁵.

We verified the validity of the chosen parameterization (at long and short distances), by a direct comparison with the case of a fully optimized Jastrow factor (i.e. without parameterization). The expression in Eq. 2 can be appropriate for physical long distance behaviors of the Jastrow factor, including the one recently speculated for describing the Mott insulator, and containing a long range $\log(R_{ij})$ term³⁶.

The Slater determinant is obtained with $N/2$ molecular orbitals $\psi_j(\mathbf{r})$, each doubly occupied by opposite spin electrons. The orbitals $\psi_j(\mathbf{r})$ are expanded in a Gaussian single-particle basis set $\{\phi_i\}$, centered on atomic nuclei, i.e. $\psi_j(\mathbf{r}) = \sum_i \lambda_{ji} \phi_i(\mathbf{r})$. The Slater determinant is build from LDA orbitals. LDA calculations are performed with a periodic Gaussian basis set (see Appendix A for its definition) by using the DFT code included in the *TurboRVB* package²⁹. This allows us to perform an efficient DFT calculation in exactly the same basis used in QMC and without employing the so called Kleinman-Bylander approximation on the PP's.

We carefully tested the effects of the basis set extrapolation on the total energy for both diamond and β -tin geometries. Following the systematically convergent method for accurate total energy calculations recently introduced in Ref.(37), we have used a tempered basis set, where the Gaussian exponents Z_i are defined as $Z_i = \alpha \beta^i$ for $i = 0, \dots, n-1$ with $\alpha = Z_{\min}$ and $\alpha \beta^n = Z_{\max}$. The parameters n , Z_{\min} and Z_{\max} are free. We verified that our basis set parameterization guarantees the same accuracy in both metallic and insulating phases for all investigated pressures.

For a given angular momentum l (≤ 4), we fixed the maximum number of Gaussians according to the formula $n_l = n_0 - 2l$, inspired by the correlated consistent basis set approach^{38,39}. It follows that the maximum number

n of exponents is used only on the s-wave channel, where $n_0 = n$. We studied the basis set extrapolation with respect to n by fixing $Z_{\min} = 0.05$ and $Z_{\max} = 10$.

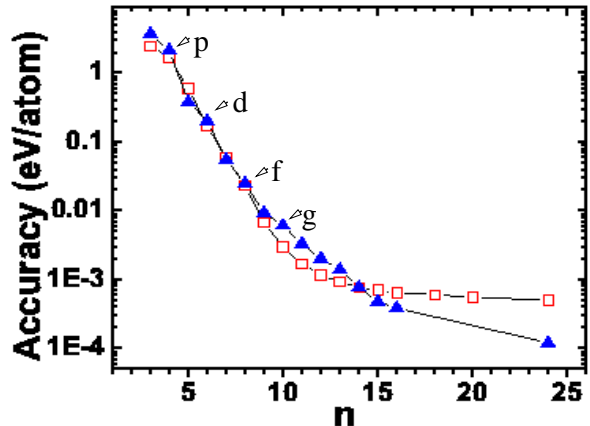


FIG. 1: Accuracy of the DFT energy as a function of the basis set extension $n(=n_0)$ defined in the text. The number of Gaussians in each angular channel l is given by $n_l = n_0 - 2l$, as explained in the text. In the plot, we indicate with an arrow the value of n when the corresponding angular channel has been switched on in the basis set expansion. The red open squares refer to the metallic β -tin phase at volume $13.081 \text{\AA}^3/\text{Si}$ and $c/a = 0.54$, while the blue triangles to the diamond insulating phase at volume $20.036 \text{\AA}^3/\text{Si}$.

In Fig. 1 we show the convergence of the DFT energy as a function of $n(=n_0)$ for a system of 8 Si atoms. We report the accuracy at $13.081 \text{\AA}^3/\text{Si}$ and $c/a = 0.54$ for the β -tin phase, and at volume $20.036 \text{\AA}^3/\text{Si}$ for the diamond phase. The accuracy in the energy is estimated by using a fully converged reference energy of a plane-wave calculation with 100 Ry kinetic energy cutoff. This was obtained with the *Qbox* package²⁸, by using the same PP's in the semilocal form as the ones used in our QMC calculations. An accuracy of 0.01 eV/Si is sufficient to determine the equation of state (EOS) with an error well below the experimental uncertainty. From this analysis it turns out that $n \geq 7$ and the inclusion of d -orbitals in the basis set guarantee an accuracy of 0.007 eV/Si on the energy difference between the two phases.

In the following, VMC and LRDMC production runs are performed using a basis set with $n_0 = 12$, $n_1 = 6$, and $n_2 = 4$. The basis set exponents have been optimized at the DFT level. We found the optimal parameters $Z_{\min} = 0.05$ and $Z_{\max} = 3.25$, that minimize the DFT energy in both the diamond and β -tin phases.

All Jastrow parameters, including exponents, are obtained by means of VMC energy minimization³⁵. Possible correlation effects not included by our Jastrow parameterization are recovered by performing LRDMC calculations. As a projector method, LRDMC allows one to obtain the best variational wave function with the same

nodal structure as the initial variational wave function, the so called fixed node approximation (FN), giving an upper bound of the true ground state energy even with non local pseudopotentials^{30,40}.

B. Finite-size errors

Contrary to standard DFT methods, QMC calculations have to be performed on a supercell. Therefore, finite size (FS) effects can be a relevant source of error in QMC calculations. Several methods have been proposed for correcting FS errors. One source of FS errors arises from the kinetic and Hartree term and can be treated by standard DFT approach with k -point sampling. This is a genuine one-body contribution, and can be corrected by $E^{\text{DFT}} - E_N^{\text{DFT}}$, i.e. the difference between the DFT energy per atom with a fully converged k -point mesh and the energy per atom of the supercell with finite volume and number of electrons N .

The other source of errors (two-body terms) is related to the finite size effects of the exchange and correlation (XC) functionals, not explicitly included in E_N^{DFT} . We calculate the two-body term corrections using the functional proposed by Kwee, Zhang and Krakauer (KZK)²³. In Ref. 23 the authors proposed to estimate this type of FS error within the LDA framework, where the exchange and correlation energy functional is replaced by the LDA functional parameterized for a finite system, which keeps an explicit dependence on the number of particles. Therefore, the total one- and two-body correction is given by $\Delta^{\text{KZK}} = E^{\text{DFT}} - E_{N,\text{KZK}}^{\text{DFT}}$, where $E_{N,\text{KZK}}^{\text{DFT}}$ is the DFT energy computed with the KZK functional for N electrons.

We observe that FS errors can be particularly relevant for open shell metallic systems. The AGP wave function approach allows to include many determinants in a effective way, removing the degeneracy of the open shell by an appropriate fractional occupation of the degenerate levels. Within LDA, by using a negligible smearing in the occupation of the KS energy levels, the degenerate orbitals containing the HOMO are partially occupied with the same charge, and can be used consistently in the AGP wave function.

For alleviating the effects of the one-body terms, we performed VMC and LRDMC calculations averaging the KZK corrected energies over the two most symmetric points (Γ and M). Previous DMC calculations^{13,18} were performed only at the Γ point, leading to more pronounced size effects. In Tab. I we report the energy for different sizes together with KZK corrections, while in Fig. 2 we show how important is to average over the Γ (PBC) and M (APBC) points to reduce considerably the error in the finite size extrapolation⁵⁷. By averaging over PBC and APBC boundary conditions we reach an accuracy of 5 meV/atom with 64 atoms, well below the magnitude of other systematic errors, as we will see in Sec. III. Therefore, at variance with Ref. 13, where a

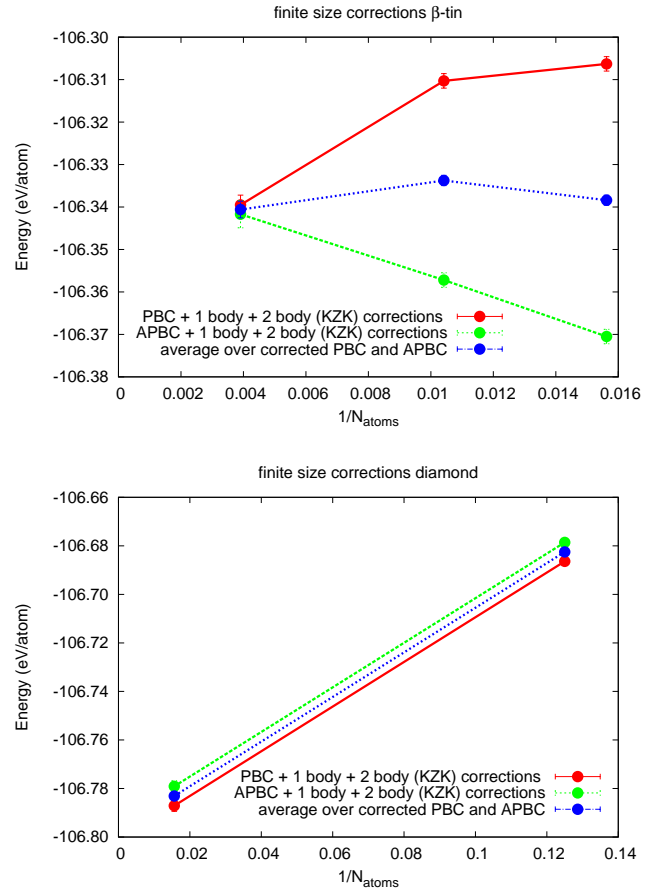


FIG. 2: Finite size extrapolation for the β -tin ($V = 15 \text{ \AA}^3/\text{Si}$, $c/a=0.55$) and the diamond ($V = 19.949 \text{ \AA}^3/\text{Si}$) phases in the upper and lower panel, respectively. The data points correspond to the values reported in Tab. I, obtained with the Trail-Needs pseudopotentials. In the plot the energy per atom is shown as a function of $1/N_{\text{atoms}}$, where N_{atoms} is the number of Si in the crystal supercell. Note the slopes for a given boundary condition (either PBC or APBC) in the two cases differ by a factor of 10, making the extrapolation much harder for the metallic phase.

single k -point was adopted in the size extrapolations, the finite size bias is not the largest error in our calculations.

III. IMPACT OF VARIOUS APPROXIMATIONS

A. Pseudopotential approximation

The change in Silicon coordination number (from 4 to 6), related to the structural transition from diamond to β -tin geometries, may affect the transferability of Si PP's in the two phases.

We verified the impact of PP's on our final results, by estimating the transition pressure at the DFT-LDA level with different norm conserving PP's and with the projector augmented-wave (PAW) method^{41,42, 58}. The results

N_{atoms}	$E_{\text{PBC}}^{\text{QMC}} + \Delta_{\text{PBC}}^{\text{KZK}}$	$\Delta_{\text{PBC}}^{\text{KZK}}$	$E_{\text{APBC}}^{\text{QMC}} + \Delta_{\text{APBC}}^{\text{KZK}}$	$\Delta_{\text{APBC}}^{\text{KZK}}$	$(E_{\text{PBC}}^{\text{QMC}} + E_{\text{APBC}}^{\text{QMC}} + \Delta_{\text{PBC}}^{\text{KZK}} + \Delta_{\text{APBC}}^{\text{KZK}})/2$	$(\Delta_{\text{PBC}}^{\text{KZK}} + \Delta_{\text{APBC}}^{\text{KZK}})/2$
64 β -tin	-106.3063(17)	-.0654	-106.3705(17)	.2214	-106.3384(12)	.07799
96 β -tin	-106.3103(17)	-0.0584	-106.3572(20)	0.0865	-106.3338(13)	0.01409
256 β -tin ^a	-106.3395(23)	-.0273	-106.3417(32)	.08855	-106.3406(22)	.03064
64 diamond	-106.7871(23)	-0.0329	-106.7791(23)	-0.0044	-106.7831(16)	-0.0187
8 diamond	-106.6864(14)	-.6700	-106.6786(14)	-.6632	-106.6825(10)	-0.6666

TABLE I: Energy per atom (in eV) for various system sizes in the metallic β -tin ($V = 15 \text{ \AA}^3/\text{Si}$, $c/a=0.55$) and insulating diamond ($V = 19.949 \text{ \AA}^3/\text{Si}$) phases with the Trail-Needs pseudopotentials. $E_{(\text{A})\text{PBC}}^{\text{QMC}}$ is the variational QMC energy with the given PBC or APBC boundary conditions. $\Delta_{(\text{A})\text{PBC}}^{\text{KZK}}$ is the total one-body and two-body correction computed by means of the KZK energy functional, with the same boundary conditions.

^a Corrected by $-0.0082(13)\text{eV/atom}$ to take into account that in this case for the long distance tail of the Jastrow a few variational parameters ansatz was adopted, as described in Sec. II A. The same form was used in the 64-Si case to estimate this correction.

have been compared with all electron calculations obtained with the Wien2k²⁷ code. In Fig. 3, we report the EOS obtained with norm conserving PP's generated by the Troullier-Martins method with scalar relativistic corrections and different cutoff radii r_c , the data obtained by the PAW method, and the reference all-electron results. The PP DFT calculations have been done with the PWSCF code²⁶. We worked with a plane wave cutoff of 50 Ry and a charge density cutoff of 200 Ry. The number of non-equivalent k-points in the Brillouin zone is 160 for the β -tin phase, and 80 for the diamond structure. We checked that those parameters give converged DFT results with a Gaussian broadening of 0.01 Ry of the Fermi surface.⁴³ On the other hand, the Wien2k calculations are PP error free, and therefore they can be used to check the PP accuracy. They have been performed with an equivalent Brillouin zone integration over a $17 \times 17 \times 17$ k-point mesh, a muffin-tin radius $R_{\text{MT}} = 1.90 a_0$ (a_0 is the Bohr radius), and a plane wave cutoff k_{max} given by $R_{\text{MT}}k_{\text{max}} = 10$. These parameters give converged results. If the error from the PP approximation were negligible, all EOS curves would superimpose on each other. Instead, Fig. 3 shows that the EOS differ significantly. As reported in Tab. II, the transition pressure seems to converge with respect to the Troullier-Martins core radius as it gets small. Its main effect is to shifts the relative position between the diamond and β -tin EOS branches. The EOS from PP's calculations are however different from the all-electron one, even for the smallest r_c . Our results clearly show how the prediction of properties under pressure is affected by the PP approximations. The best choice in the DFT framework is to use the PAW pseudopotentials, which give both the transition pressure and EOS very close to the all-electron results.

At the QMC level additional errors may come from the lack of a consistent method to generate PP's from the corresponding correlated QMC calculation for an isolated atom⁵⁹. A direct evaluation of the core-valence interaction was attempted in Ref.18.

In Tab. III we report our VMC and LRDMC results using Hartree-Fock, energy adjusted and LDA generated pseudopotentials. The transition pressures reported in

DFT method	p_t (GPa)
LDA LAPW	7.12
LDA PW PAW	7.21
LDA PW Troullier-Martins $r_c = 1.67 a_0$	7.44
LDA PW Troullier-Martins $r_c = 2.2 a_0$	7.65
LDA PW Troullier-Martins $r_c = 2.6 a_0$	8.27

TABLE II: DFT transition pressures for different pseudopotentials in PWSCF calculations and all-electron Wien2K LAPW calculations done with the LDA functional. Note the convergence of the Troullier-Martins pseudopotential with respect to the core radius r_c . By using soft pseudopotentials, the error could be of 1 GPa on the final transition pressure. The best DFT pseudopotential is the PAW one, with a final transition pressure within 0.1 GPa from the all-electron result.

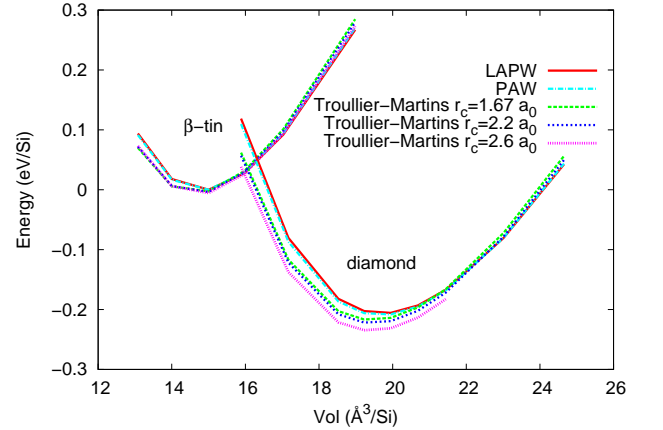


FIG. 3: EOS obtained by DFT LDA calculations with PWSCF and LAPW methods. The PP's in the PW formalism have been generated by the Troullier-Martins scheme with the cutoff radius r_c reported in the figure key. The zero of the energy has been chosen to be the minimum of the β -tin EOS, corresponding to the volume $V = 15 \text{ \AA}^3/\text{Si}$. This choice helps the comparison among the EOS curves. Note that the PWSCF calculations done with the PAW pseudopotential are on top of the all-electron LAPW points.

pseudopotential	VMC	LRDMC
HF Trail-Needs	15.48(6)	16.65(15)
energy adjusted Burkatzki-Filippi-Dolg	15.80(6)	16.50(12)
LDA Troullier-Martins $r_c = 1.67 a_0$	15.39(18)	16.83(19)
LDA Troullier-Martins $r_c = 2.1 a_0$	15.08(18)	16.11(19)

TABLE III: Transition pressures for different pseudopotentials in VMC and LRDMC calculations. Calculations are done at volume per atom of 13.08 \AA^3 and 19.95 \AA^3 for the diamond and β -tin phase respectively, and the Maxwell construction done assuming for the EOS the same curvature as in the Trail-Needs case, fully resolved with respect to its volume dependence. r_c is the cutoff radius in the pseudopotential generation scheme. The factor used to convert energy differences into pressures is 26.812 GPa/eV .

Tab. III are evaluated by computing the energy of the diamond and β -tin phase at the volume per atom of 13.08 \AA^3 and 20.69 \AA^3 respectively, and assuming that the curvature of the corresponding EOS is the same as the one computed for the Trail-Needs pseudopotentials.

Results in Fig. 3 and Tab. III clearly shows the interaction between core and valence electrons cannot be approximated by a rigid shift in energy (as usually assumed estimating the effect of PP on the transition pressure).

Core-valence interactions accounts for a correction of $1.2 \pm 0.6 \text{ GPa}$ and were calculated in Ref. 18. In order to improve the accuracy of this correction an all electron calculation is required. At present this is almost impossible within QMC, and therefore an uncertainty of at least 1 GPa coming directly from the PP approximation is unavoidable in our QMC findings.

B. Phonons and temperature effects

The inclusion of finite temperature and zero point motion effects is crucial for a direct comparison of our results with finite temperature experiments (usually performed at room temperature). Both experiments⁴⁴ and theory¹⁴ indicate that temperature corrections induce a positive shift to the critical equilibrium line. On the other hand, a further shift in pressure is induced by the inclusion of zero point motion effects. Phonon dispersions are in fact different in the two phases and zero point motion effects do not compensate.

Finite temperature effects and zero point motion energies are included in our estimate of the transition pressure, by calculating phonon dispersions for the β -tin and diamond phase with the QE package. In order to study the convergence of our phonon calculations with the k-point mesh we performed PWSCF runs with large plane wave cutoff (up to 100 Ry), accurate k-point sampling (up to 1620 inequivalent k-points for the β -tin phase and 480 inequivalent k-points for the diamond phase), as well as a small value of the Gaussian broadening (width of 0.0001 Ry). We have used the PAW data set as in the previous section for the LDA calculation, and an ultra-

soft (US) PP generated with similar parameters and core radii for the PBE calculation.

Following Ref. 14, we compute the harmonic correction ΔF to the free energy per atom, by using the phonon density of states $D(\omega)$ available in QE after Fourier interpolation of the phonon bands, (namely by using `matdyn.x`):

$$\Delta F = kT \int_0^\infty d\omega D(\omega) \ln \left(2 \sinh \left(\frac{\omega}{2kT} \right) \right) \quad (4)$$

where $\hbar = 1$ is assumed. In using the above expression, one has to take into account that the total phonon density of states per atom is obviously normalized to

$$\int_0^\infty d\omega D(\omega) = 3 \quad (5)$$

as there are three phonon modes per atom in the thermodynamic limit. Integrations were changed to summations over a uniform mesh with high resolution (1 cm^{-1}), and the original density of states was appropriately scaled to fulfill Eq. 5.

Free energy corrections (see Tab. IV) are then added to a total energy zero temperature calculations. In this way our calculation of the transition pressure, estimated by the Maxwell construction of the free energy curves, is essentially free of systematic errors within the chosen DFT functional, as long as phonon anharmonic effects can be neglected in the low temperature regime. This is a reasonable assumption below the melting temperature occurring at about $\simeq 1000 \text{ K}$.

To test the impact of the exchange and correlation functional on quantum correction estimates, we have performed calculations with both the PBE and LDA functionals. As shown in Fig. 4, although different functionals provide different transition pressures, the corrections to the bare values are very similar and consistent within 0.2 GPa and in fair agreement with experimental results. The results demonstrate that phonons are rather well described within DFT and these corrections are very reliable at least before the melting point. Our results do not agree with a previous work¹⁴ on this subject, where the zero temperature quantum corrections were underestimated by about a factor two, and finite temperature corrections were larger by about a factor three. PP used in Ref.14 is no more available and we were not able to reproduce the quoted results. Presently the reason for this discrepancy is not clear.

With new available PP's, our temperature corrections are very well converged, and appear in reasonable agreement with recent experimental data (see Fig. 4).

By using DFT-PBE free energy corrections to VMC total energies, we obtain the corrected VMC curve reported in Fig. 5, and the corrected transition pressures in Tab. V. As one can note, the zero point energy for the diamond phase is larger than the one for the β -tin

V ($\text{\AA}^3/\text{Si}$)	0K	100K	300K	500K	700K	1000K
Diamond phase						
15.882	0.077/0.073	0.073/0.069	0.042/0.039	-0.012/-0.016	-0.084/-0.090	-0.218/-0.226
17.169	0.069/0.068	0.067/0.066	0.040/0.041	-0.012/-0.011	-0.083/-0.081	-0.215/-0.212
18.524	0.066/0.064	0.064/0.063	0.039/0.038	-0.012/-0.014	-0.082/-0.084	-0.213/-0.216
19.228	0.064/0.062	0.062/0.061	0.038/0.036	-0.014/-0.016	-0.084/-0.087	-0.216/-0.220
19.949	0.062/0.060	0.060/0.059	0.036/0.034	-0.017/-0.019	-0.088/-0.091	-0.221/-0.225
20.687	0.060/0.058	0.058/0.057	0.033/0.031	-0.020/-0.022	-0.092/-0.095	-0.226/-0.231
21.444	0.058/0.056	0.056/0.055	0.031/0.029	-0.023/-0.026	-0.096/-0.101	-0.233/-0.238
23.013	0.054/0.052	0.052/0.051	0.025/0.023	-0.032/0.034	-0.108/0.112	-0.249/0.254
24.656	0.050/0.048	0.048/0.047	0.019/0.017	-0.040/0.044	-0.120/0.124	-0.265/0.271
β -Sn phase						
13.081	0.055/0.053	0.053/0.051	0.025/0.022	-0.033/0.036	-0.110/0.114	-0.251/0.257
14.004	0.049/0.047	0.048/0.046	0.017/0.014	-0.044/0.048	-0.125/0.130	-0.272/0.280
15.000	0.044/0.042	0.042/0.040	0.008/0.005	-0.058/0.063	-0.144/0.150	-0.299/0.308
15.978	0.039/0.037	0.036/0.035	-0.002/0.005	-0.073/0.078	-0.164/0.172	-0.328/0.339
17.031	0.034/0.032	0.030/0.028	-0.014/0.019	-0.093/0.100	-0.192/0.202	-0.368/0.382
18.984	0.026/0.025	0.020/0.019	-0.037/0.040	-0.129/0.135	-0.242/0.250	-0.438/0.450

TABLE IV: Finite temperature corrections to the free energy (eV/atom) within PBE/LDA DFT theory, as explained in the text.

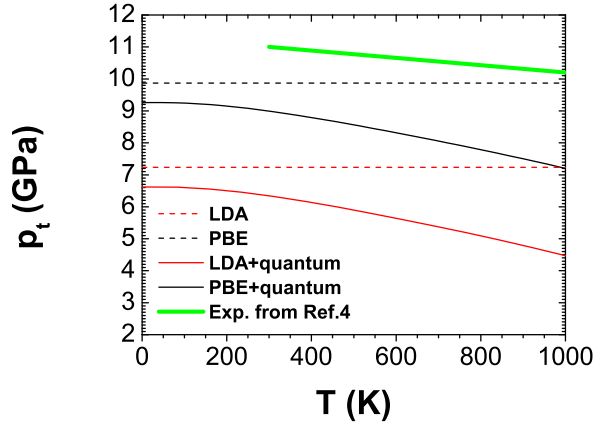


FIG. 4: Effect of harmonic quantum corrections on the transition pressure in Silicon as a function of temperature.

	VMC p_t	LRDMC p_t
Born-Oppenheimer	15.48(6)	16.65(15)
zero point motion	14.84(6)	15.71(14)
$T = 300$ K	14.53(6)	15.74(17)

TABLE V: Transition pressures p_t in VMC and LRDMC calculations with quantum and temperature effects. The values are obtained by a Maxwell construction on a cubic fitting of the EOS, corrected at each volume by the DFT-PBE estimates.

phase by ≈ 0.2 eV, which decreases the transition pressure by 0.65 GPa. The finite temperature correction is negative, and its absolute value is larger for the β -tin phase. Therefore, a further reduction of 0.30 GPa is obtained at 300K, which implies that the total correction at room temperature is 0.95 GPa, a smaller value than the

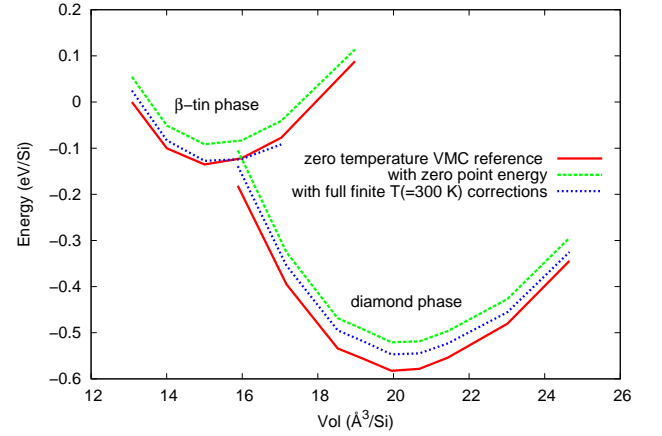


FIG. 5: The corrected equation of state once the zero point energy and the temperature effects are added (estimated at the DFT-PBE level). The reference is the VMC calculation reported in Fig. 7, and here the zero of energy is taken as the VMC value at $V = 13.08 \text{ \AA}^3/\text{Si}$.

one estimated in Ref. 14. At the LRDMC level, we obtain roughly the same total correction (0.91 GPa), although it is more difficult to discriminate the temperature effect, as the statistical error is larger (see Tab. V).

C. Kleinman-Bylander approximation

The matrix elements of the non-local PP can be evaluated either by direct numerical Gauss-Hermite (GH) integration over the polar coordinates or by using the Kleinman-Bylander (KB) approximation^{45,46}. The KB approach is a rather general concept, and it is applied in DFT calculations to make the calculation of the PP operator more efficient. In particular, in the plane-wave

formalism the generated PP is conveniently expressed in the plane-wave basis set. On the other hand, in the QMC framework, one usually works in the coordinate representation where electron positions and spins are given, and this makes the KB construction hard to implement numerically. Consequently, the pseudopotentials used in QMC are usually generated in the so called semilocal form (local + non local part), and computed by performing a random integration over their angular components^{30,47,48}. However, in previous QMC calculations of the Si diamond-to- β -tin transition^{13,18} the determinantal part has been generated from plane-wave DFT calculations, where the KB approximation was used⁴⁹ to represent a pseudopotential originally written in a semilocal form. This procedure could lead in principle to a poorer form of the variational wave function in the proximity of the core, where the non-local PP is mostly localized, with an impact on its nodal structure, and therefore a larger FN error.

To investigate the impact of KB approach, we compared the total energy, the kinetic energy, and the non-local term of the PP, obtained from a single M-point DFT calculation with and without the KB approximation. The results are shown in Tab. VI for a system of 8 Si in the β -tin phase with $c/a = 0.54$ and volume $13.081 \text{ \AA}^3/\text{Si}$, and in the diamond phase with volume $20.036 \text{ \AA}^3/\text{Si}$. Calculations within the KB approximation are done using the *PWscf* DFT implementation²⁶. We use the *Qbox* code²⁸ for performing plane-wave calculations with Gauss-Hermite integration. An energy cut-off of 100 Ry was used in all the plane-wave calculations. The exchange and correlation energy was described in the LDA by the Perdew-Zunger functional⁵⁰. The energies reported in Tab. VI and Tab. VII clearly show that the use of KB approximation causes an error of 0.3 eV/Si when evaluating the contribution from the non-local term of the PP. This error cancels out in the energy difference between the two phases, leaving the DFT results unbiased by this kind of approximation. In principle, our analysis cannot exclude that the nodal structure of the DFT generated wave function is unaffected close to the core, since there is a significant KB error in the PP contribution of the total energy. In practice, the close agreement between our LRDMC results, unaffected by the KB approximation, and the ones in Ref. 13, where this approximation has been used, shows that the cancellation of KB errors applies also in QMC calculations and leads to unbiased energy differences.

Our results are unaffected by the KB approximation by construction, as the DFT code implemented in the *TurboRVB* package uses the exact GH integration of the semilocal pseudopotentials. Moreover, the DFT results shown in Tab. VI and Tab. VII are a further validation of the convergence of our periodic Gaussian basis set. Indeed, we found a perfect agreement between the energies obtained with plane-wave calculations (performed by means of the *Qbox* code²⁸ and without the KB approximation) and the ones obtained with our Gaussian

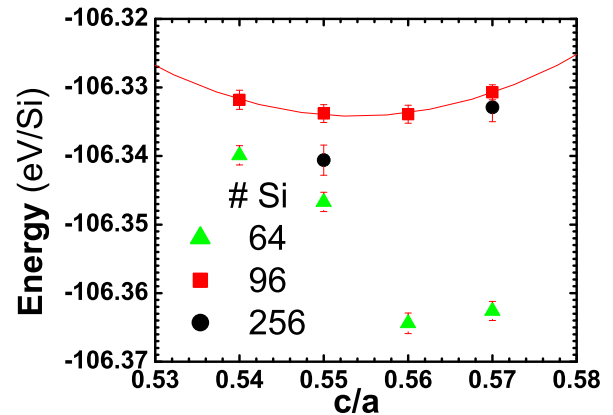


FIG. 6: Energy vs c/a in the β -tin phase at fixed volume $15 \text{ \AA}^3/\text{Si}$ for various sizes. FS corrections from the KZK extrapolation are included and energies are averaged over the two most symmetric points (Γ and M) of the Brillouin zone. In the largest size the Jastrow factor was parameterized at large distance according to Eq.(2) and the error of the restricted variational freedom ($\simeq -0.0082 \text{ eV/atom}$) was estimated with the same calculation for 64 Si atoms.

basis set implementation in the *TurboRVB* package²⁹.

IV. RESULTS

In this section we present our QMC results for the transition pressure, performed with the Trail-Needs pseudopotentials. We first validate the quality of our variational wave function in both the β -tin and diamond phases. In the β -tin phase, we compute the c/a ratio in the proximity of the critical pressure (at volume $V = 15 \text{ \AA}^3/\text{atom}$), where this lattice parameter is experimentally known. We evaluate also the bulk modulus and other structural properties from the fit of the equation of state $E = E(V)$, and compare them with former experimental and theoretical values. Finally, we compute the transition pressure by performing the Maxwell construction on the EOS of both phases.

In Fig. 6 we report the VMC energies as a function of the c/a ratio for the β -tin phase at different supercell size (64, 96, 256 Si atoms) and fixed volume $V = 15 \text{ \AA}^3/\text{atom}$. All the energies include FS corrections within the KZK scheme, as reported in Subsec. II B. The results in Fig. 6 are a first test of the quality of our WF for describing the β -tin phase. With the Jastrow optimization we reproduce rather well the experimental value $c/a = 0.554$. Therefore for all the following VMC and LRDMC calculations we fix the c/a ratio to the value 0.55.

In Fig. 7 we reported the VMC results for the energy $E(V)$ as a function of the volume V . All the energies in the Figure include FS corrections using the KZK scheme. Although FS effects are more pronounced in the metallic

Quantity	KB	GH	present $n = 24$	present $n = 10$
Total energy	-102.85692	-102.84036	-102.83975	-102.83737
Kinetic energy	50.95461	50.83712	50.83563	50.83195
Non-local pseudo	22.13269	22.45092	22.45256	22.45398

TABLE VI: Comparison of LDA-DFT energies (eV/Si) obtained within the KB approximation and with the GH numerical integration over the polar coordinates of non-local PP matrix elements. We report the total energy, the kinetic energy and the non-local contribution of the PP for a system of 8 Si with anti periodic boundary conditions (M -point) in the β -tin phase with $c/a = 0.54$ and volume $13.081\text{\AA}^3/\text{Si}$ and Trail-Needs pseudopotentials. Calculations within the KB approximation are performed with *PWscf* code. Plane-wave calculations with a GH numerical integration are done using *Qbox* code. We report also the energies obtained for the same system using the Gaussian basis set implementation of the LDA-DFT method coded in the *TurboRVB* package (referred to as “present” in the table). n indicates the number of Gaussians for single-particle orbitals with the s symmetry.

Quantity	KB	GH	present $n = 24$	present $n = 10$
Total energy	-105.32986	-105.31911	-105.31880	-105.31302
Kinetic energy	44.0823	43.96216	43.96152	43.95454
Non local pseudo	21.43672	21.79496	21.79506	21.79468

TABLE VII: Same as in Tab. VI but for a system of 8 Si with anti periodic boundary conditions in the diamond phase at volume $20.036\text{\AA}^3/\text{Si}$.

phase, the results for the β -tin phase clearly show that the FS errors are under control. In fact we find that the energies for the 256 atoms supercell fall on the top of the data for the 64 atoms calculations. LRDMC energies are shown in Fig. 8 for 64 atoms supercell. VMC and LRDMC EOS are fitted using a cubic polynomial function. The results for bulk properties of the diamond phase, reported in Tab. VIII, are in very good agreement with the experimental values, whereas the ones for the β -tin structure compares well with previous QMC data. Note also that there exists a sizable zero point motion correction to both the equilibrium volume and the bulk modulus, that has not been taken into account so far in previous works. We have estimated these corrections by adding to the EOS the zero temperature quantum corrections evaluated within the harmonic approximation and the PBE functional, as explained in Subsec. III B.

The critical pressure of the diamond to β -tin transition is reported in Tab. IX. VMC calculations give a raw p_t of $15.48(6)$ GPa, LRDMC data give $16.65(15)$ GPa.

The inclusion of zero point motion, finite temperature and core-valence contributions bring the transition pressure to $13.33(70)$ GPa (VMC) and $14.50(70)$ GPa (LRDMC), for a total final shift of -2.15 GPa (Tab. IX). Zero point motion and thermal corrections at 300 K amount to -0.65 GPa and to -0.3 GPa respectively (they are estimated performing a PBE phonons calculations, as explained in Subsec. III B). The core-valence interaction contribution is -1.20 ± 0.6 GPa from Ref. 18, the same value has been used in Refs. 13,18,20. Contributions beyond frozen core approximation are already included at the DFT level through non-linear core corrections in the PP. We observe that previous calculations^{18,2013} consider a total correction to the raw data of -2.5 GPa, because of the different value of the zero point energy and finite temperature effects. All previous calculations should be increased by 0.35 GPa, for

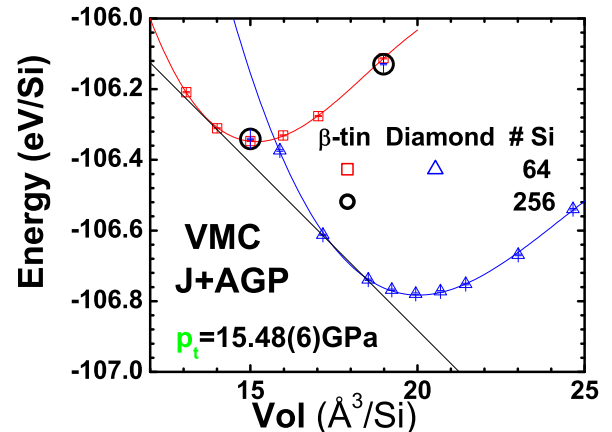


FIG. 7: Equation of state and the metal-insulator transition pressure in bulk Silicon obtained by the VMC technique after optimizing a Jastrow factor in a localized basis set containing $2s$ and $2p$ Gaussian orbitals per Si. The energies are corrected using the KZK correction scheme.²³ In this way finite size effects of the transition pressure appears to be small. The lattice value $c/a = 0.55$ is used for the β -tin phase. The data plotted here are not yet corrected for the quantum and temperature effects. See Tab. IX for the final pressure which includes zero point motion and thermal contributions.

accounting this difference. .

Both our corrected VMC and LRDMC values are above the experimental range, and remarkably the more accurate LRDMC method leads to a transition pressure p_t larger than the VMC result.

To further support the accuracy of our LRDMC calculations, we have systematically optimized the molecular orbitals by minimizing the VMC energy in presence of

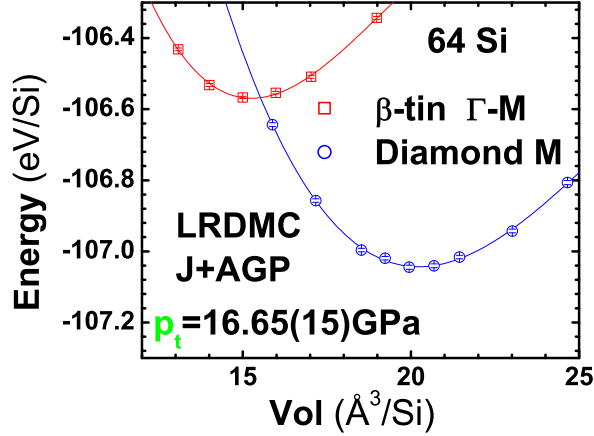


FIG. 8: The same as in Fig. 7 but for the LRDMC calculations.

a Jastrow factor, starting from the LDA orbitals, for a system of 8 Silicon atoms (see Tab.X). The optimization of the molecular orbitals allows us to assert the impact of the wave function on the final LRDMC results.

We have found that the LDA orbitals are a quite accurate starting point, but for the diamond at equilibrium geometry the total VMC energy decreases slightly more ($\simeq 0.01\text{eV/atom}$) than the one for the β -tin at high pressure, implying an increase in the transition pressure of about 0.4 GPa at the VMC level. That is again consistent with the more accurate LRDMC calculation, which is much less affected by the optimization of the wave function as clearly shown in Tab. X. Altogether these results point even more clearly in the direction of a larger zero temperature transition pressure.

V. CONCLUSIONS

We have performed DFT and QMC calculations for the diamond-to- β -tin transition in Silicon. At the QMC level we have proven that it is possible to accurately and efficiently describe correlation effects across the metal-insulator transition by applying a relatively simple Jastrow factor to a DFT generated Slater determinant.

We have shown that the estimation of the PP effect is one of the most delicate issues in any QMC calculation, and represents so far the most significant source of systematic error in the transition pressure, amounting to about 1GPa, as described in Subsec. III A. The core-valence correlation correction strongly depends on the PP, and is almost unpredictable without doing the corresponding all-electron calculation. Moreover, the only known QMC estimate for this correction (-1.2GPa), was done in Ref. 18 for the Trail-Needs PP, and is affected by a large statistical error ($\simeq 0.6\text{ GPa}$).

In the present work we have also found a signifi-

diamond phase	V_{eq} ($\text{\AA}^3/\text{Si}$)	E_{cohesive} (eV/Si)	B (GPa)
LDA	19.77	5.29	95.75
PBE	20.42	4.62	89.4
VMC	20.124 ± 0.036^a	4.6003 ± 0.0015^b	102.3 ± 1.4^c
LRDMC	20.33 ± 0.1^a	4.6650 ± 0.003^b	95.78 ± 3^c
DMC (Ref. 18)	20.21 ± 0.03^a	4.62 ± 0.01^b	101.4 ± 10^c
DMC (Ref. 13)	20.08 ± 0.05^a	-	98 ± 7^c
Exp.	20.0^d	4.62 ± 0.08^e	99^d
β -Sn phase	V_{eq} ($\text{\AA}^3/\text{Si}$)	E_{cohesive} (eV/Si)	B (GPa)
LDA	14.92	5.10	115.4
PBE	15.45	4.29	110.7
VMC	15.25 ± 0.05^f	4.186 ± 0.0013^g	119.7 ± 3.5^h
LRDMC	15.34 ± 0.16^f	4.211 ± 0.0024^g	111.3 ± 8.3^h
DMC (Ref. 13)	15.31 ± 0.2^f	-	98.6 ± 12^h

TABLE VIII: Comparison of present numerical results with previous QMC data and available experiments for the equilibrium properties of Silicon in the diamond structure: equilibrium volume (V_{eq}), cohesive energy (E_{cohesive}), and bulk modulus (B) are reported. They were estimated by a cubic interpolation of the $E(V)$ points. The DFT pseudopotentials used here includes non linear core polarization terms and scalar relativistic corrections and are in consistent agreement with corresponding all-electron calculations. For the DFT methods the cohesive energy is given by the magnetic solution of the single atom, whereas quantum corrections are included according to Tab.(IV). All corrections to QMC data are estimated within the DFT-PBE functional. We have also checked that standard LDA functional provides similar corrections.

^aCorrected by $0.1\text{\AA}^3/\text{atom}$ to take into account the zero point motion.

^bCorrected by -0.06eV/atom to take into account the zero point motion.

^cCorrected by -1.6GPa to take into account the zero point motion. VMC and LRDMC are further corrected by -10 GPa to take into account non cubic terms in the interpolation within the equilibrium volume range $13 \leftrightarrow 19$ ($16 \leftrightarrow 25$) $\text{\AA}^3/\text{atom}$ in the β -tin (diamond) phase.

^dTaken from Ref. 51

^eTaken from Ref. 52

^fCorrected by $0.11\text{\AA}^3/\text{atom}$ to take into account the zero point motion.

^gCorrected by -0.04eV/atom to take into account the zero point motion.

^hCorrected by -2.8GPa to take into account the zero point motion. VMC and LRDMC are further corrected by -5.6GPa analogously to the diamond phase.

cant reduction of the phonon correction to the transition pressure- from the quoted -1.3 GPa^{14} to our fully converged LDA and PBE value of -0.95 GPa at 300K. This shifts up all previous QMC p_t estimates by $\approx 0.35\text{ GPa}$. Thus, we arrive at the conclusion that *all* Monte Carlo findings published so far predict a transition pressure that is significantly larger than the one observed at room temperature, from $1/2\text{ GPa}^{20}$ to 4 GPa^{18} above the experimental upper edge of 12.5 GPa .

Our VMC technique is in agreement with the value of the transition pressure recently reported by the AFQMC technique²⁰. A clear increase of the transition pressure by about 1GPa is obtained when the accuracy of the cal-

method	raw (GPa)	corrected (GPa) ($T = 300$ K)
LDA	7.21	6.34
PBE	9.87	8.99
VMC	15.48 \pm 0.06	13.33 \pm 1.0
LRDMC	16.65 \pm 0.15	14.50 \pm 1.0
DMC (Ref. 18)	19.0 \pm 0.5	16.5 \pm 0.5
DMC (Ref. 13)	16.5 \pm 1.0	14.0 \pm 1.0
AFQMC (Ref. 20)	15.1 \pm 0.3	12.6 \pm 0.3
Exp.	10.0 - 12.5	10.0 - 12.5

TABLE IX: Zero temperature transition pressure in GPa obtained by a cubic interpolation of the EOS. Comparison of the present numerical results with available experiments and previous theoretical data. The corrected numerical QMC data are obtained after including the zero point motion, finite temperature, and core-valence contributions, which are not present in the raw data, as explained in the text. DFT corrections include only the zero point motion and finite temperature effects as they are performed with the non-linear core correction in the pseudopotentials. In particular, the LDA results have been obtained by using a PAW PP, while the PBE values come from an US PP. For the core-valence contributions we have used the published DMC estimate in Ref.18, that unfortunately is affected by a very large error bar, as discussed in the text. The raw data and the corrections applied by other authors have been taken from the referenced papers.

culution is improved by the LRDMC scheme. Although LRDMC total energies are more accurate, it is in principle possible that this technique could lead to results worse than the VMC ones in the estimation of the equation of state. However we believe that this is quite unlikely, because DMC as well as LRDMC always improve the accuracy of the physical estimates, as long as they are applied to a reasonably good variational wave function.

As a further independent check that a more accurate transition pressure is larger than the VMC estimate, we have optimized the Slater determinant in presence of the Jastrow factor for a small number of atoms, and found a consistent increase in the transition pressure. Although we cannot estimate more accurately the nodal error -namely the exact ground state result for given pseudopotential- it looks plausible that by fully optimizing the wave function this error should decrease. Therefore, our orbital optimization should give at least the trend of the correction to the approximate VMC result.

On the other hand, our LRDMC result is very close to the recent DMC calculation performed by Hennig *et al.*¹³, where the same pseudopotential was used,

whereas the DFT Slater determinant was obtained with the PBE functional and the KB approximation for the pseudopotential⁴⁹. This agreement suggests also that the DMC/LRDMC technique is weakly dependent on the functional used to generate the DFT orbitals and should be considered rather accurate for a given pseudopotential.

To summarize, our best estimate of the transition pressure at room temperature is 14.5 GPa, with an uncertainty of 1 GPa coming mainly from the pseudopotential approximation, as our finite-size extrapolation error is definitely smaller. The discrepancy with respect to the experimental values leads us to conclude that further work is necessary to determine the phase boundary of the metal-insulator transition in Silicon. On one hand, from the experimental point of view one should verify whether, by removing the stress anisotropy in the experimental environment, the transition pressure can significantly increase and get closer to the QMC prediction, as suggested in Ref. 13. On the other hand, in QMC calculations it should be worth defining consistent pseudopotentials, since we have seen that they can significantly affect the EOS at large pressure. So far there is in fact no accurate method to estimate the systematic error related to the pseudopotential approximation, since an all-electron calculation of bulk silicon is basically prohibitive within the QMC method. A first attempt along these lines has been done in Ref. 53. At this stage of development the construction of pseudopotentials is quite unsatisfactory for high accuracy QMC calculations, since the pseudopotentials are usually determined with different and less accurate techniques, as Hartree-Fock or LDA. Despite the recent progress in the use of pseudopotentials within DMC^{30,40,54}, the implementation of the pseudopotential approximation in the many-body QMC framework is not as mature as in the DFT, where a remarkable progress was made only after several years of experience with the so called PAW method^{41,42}. Thus, in QMC we believe there is room for a significant improvement to be realized in the next years.

Appendix A: Gaussian periodic basis set

We use a localized Gaussian basis set on a box of lengths L_x, L_y, L_z , defining the periodic electron-ion distance as

$$r_{iJ} = \sqrt{\left(\frac{L_x}{\pi} \sin\left(\frac{\pi}{L_x}(x_i - X_j)\right)\right)^2 + \left(\frac{L_y}{\pi} \sin\left(\frac{\pi}{L_y}(y_i - Y_j)\right)\right)^2 + \left(\frac{L_z}{\pi} \sin\left(\frac{\pi}{L_z}(z_i - Z_j)\right)\right)^2} \quad (\text{A1})$$

where x_i, y_i, z_i indicate the Cartesian components of the electron coordinates \mathbf{r}_i for $i = 1, \dots, N$ and X_j, Y_j, Z_j

the corresponding ion ones \mathbf{R}_j with $j = 1, \dots, N_A$. The

system	DFT+J/LRDMC	FOPT/LRDMC
diamond $V = 19.949\text{\AA}^3/\text{Si}$ PBC	-106.0120(12)/-106.3064(27)	-106.0493(10)/-106.3204(24)
β -tin $V = 13.081\text{\AA}^3/\text{Si}$ PBC	-106.5557(11)/-106.8765(28)	-106.5890(10)/-106.8871(32)
β -tin $V = 13.081\text{\AA}^3/\text{Si}$ APBC	-103.7359(13)/-104.0720(41)	-103.7617(9)/-104.0818(36)

TABLE X: Variational Monte Carlo/LRDMC energy per atom (eV) for a system of 8 Si with periodic (PBC) and antiperiodic (APBC) boundary conditions obtained with the same basis: 8s6p4d for the Slater determinant, and 2s2p/1s1p for the Jastrow factor. In the DFT+J case only the Jastrow factor (with no restriction to the exponents of the Gaussians) is optimized, while the determinantal part is the output of an LDA calculation in the 8s6p4d basis. Conversely, in the fully optimized (FOPT) case the molecular orbitals are optimized together with the Jastrow factor, while keeping fixed the exponents of the 8s6p4d Gaussians to the even tempered values discussed in the text (see Subsec. IIA).

angular part of the Gaussian basis can be defined in strict analogy with the conventional scheme for open systems. They are obtained by multiplying the overall Gaussian $\exp(-Zr_{iJ}^2)$ by appropriate polynomials of $\sin(\frac{\pi}{L_\mu}\mathbf{r}_{iJ}^\mu)$ and $\cos(\frac{\pi}{L_\mu}\mathbf{r}_{iJ}^\mu)$, where $\mathbf{r}_{iJ}^\mu = \mathbf{r}_i^\mu - \mathbf{R}_J^\mu$ and $\mu = x, y, z$ labels the three Cartesian components. Strictly speaking in the periodic case there is an arbitrariness in defining this polynomials because the multiplication of a polynomial by any even cos-power defines an allowed element of the atomic basis satisfying the periodic or antiperiodic boundary conditions in each direction.

In order to define the basis in an accurate and convenient way, we have chosen the unique polynomials that contain the minimum possible cosine powers. For instance the angular part $Y_{l=2,m}r^2$ of the d -wave orbital is defined by:

$$\text{for } m = 0 : \quad (\text{A2})$$

$$\frac{1}{2} \left(3 \left(\frac{L_3}{\pi} \sin\left(\frac{\pi}{L_3}\mathbf{r}^3\right) \right)^2 - r^2 \right)$$

$$\text{for } m = \pm 1 : \quad (\text{A3})$$

$$\sqrt{3} \frac{L_2}{\pi} \sin\left(\frac{\pi}{L_2}\mathbf{r}^2\right) \cos\left(\frac{\pi}{L_2}\mathbf{r}^2\right) \frac{L_3}{\pi} \sin\left(\frac{\pi}{L_3}\mathbf{r}^3\right) \cos\left(\frac{\pi}{L_3}\mathbf{r}^3\right)$$

$$\sqrt{3} \frac{L_1}{\pi} \sin\left(\frac{\pi}{L_1}\mathbf{r}^1\right) \cos\left(\frac{\pi}{L_1}\mathbf{r}^1\right) \frac{L_3}{\pi} \sin\left(\frac{\pi}{L_3}\mathbf{r}^3\right) \cos\left(\frac{\pi}{L_3}\mathbf{r}^3\right)$$

$$\text{for } m = \pm 2 : \quad (\text{A4})$$

$$\sqrt{3} \frac{L_1}{\pi} \sin\left(\frac{\pi}{L_1}\mathbf{r}^1\right) \cos\left(\frac{\pi}{L_1}\mathbf{r}^1\right) \frac{L_2}{\pi} \sin\left(\frac{\pi}{L_2}\mathbf{r}^2\right) \cos\left(\frac{\pi}{L_2}\mathbf{r}^2\right)$$

$$\frac{\sqrt{3}}{2} \left(\left(\frac{L_1}{\pi} \sin\left(\frac{\pi}{L_1}\mathbf{r}^1\right) \right)^2 - \left(\frac{L_2}{\pi} \sin\left(\frac{\pi}{L_2}\mathbf{r}^2\right) \right)^2 \right)$$

Acknowledgments

We acknowledge F. Gygi for his support in using the *Qbox* code. We thank Shiwei Zhang and Matteo Calandra for useful discussions and correspondence. We are especially in debt with Pasquale Pavone for useful comments and suggestions about the phonon calculations. MC thanks the Ecole Polytechnique, the japanese-french JST-CREST grant for financial support, and the NCSA computing facilities at the University of Illinois at Urbana-Champaign. SS was supported by MIUR COFIN07 and CINECA.

¹ R. Miletich, *EMU notes in Mineralogy: Mineral Behaviour at extreme Conditions* (7th EMU School of Mineralogy, Heidelberg, Germany, 2005).

² J. C. Jamieson, *Science* **139**, 762 (1963), ISSN 0036-8075.

³ M. I. McMahon and R. J. Nelmes, *Phys. Rev. B* **47**, 8337 (1993), ISSN 0163-1829.

⁴ G. A. Voronin, C. Pantea, T. W. Zerda, L. Wang, and Y. Zhao, *Phys. Rev. B* **68**, 020102 (2003).

⁵ J. Z. Hu, L. D. Merkle, C. S. Menoni, and I. L. Spain, *Phys. Rev. B* **34**, 4679 (1986), ISSN 0163-1829.

⁶ M. Tsujino, T. Sano, N. Ozaki, O. Sakata, M. Okoshi, N. Inoue, R. Kodama, and A. Hirose, *The Review of Laser Engineering Supplemental Volume*, 1218 (2008).

⁷ S. V. Ovsyannikov, V. V. Shchennikov, and A. Misiuk, *JETP Letters* **80**, 405 (2004).

⁸ A. Dal Corso et al., *Phys. Rev. B* **53**, 1180 (1996).

⁹ In-Ho Lee and Richard M. Martin, *Phys. Rev. B* **56**, 7197 (1997).

¹⁰ N. Moll, M. Bockstedte, M. Fuchs, E. Pehlke, and M. Scheffler, *Phys. Rev. B* **52**, 2550 (1995).

¹¹ J. P. Perdew, K. Burke, and Y. Wang, *Phys. Rev. B* **54**, 16533 (1996), ISSN 0163-1829.

¹² J. Perdew, K. Burke, and M. Ernzerhof, *Phys. Rev. Lett.* **77**, 3865 (1996).

¹³ R. G. Hennig, A. Wadehra, K. P. Driver, W. D. Parker, C. J. Umrigar, and J. W. Wilkins, *Phys. Rev. B* **82** (2010), ISSN 1098-0121.

- ¹⁴ K. Gaál-Nagy, A. Bauer, M. Schmitt, K. Karch, P. Pavone, and D. Strauch, *Phys. Status Solidi B* **211**, 275 (1999).
- ¹⁵ W. M. C. Foulkes, L. Mitás, R. J. Needs, and G. Rajagopal, *Rev. Mod. Phys.* **73**, 33 (2001), ISSN 0034-6861.
- ¹⁶ Leonardo Spanu, Sandro Sorella, and Giulia Galli, *Phys. Rev. Lett.* **103**, 196401 (2009), ISSN 0031-9007.
- ¹⁷ J. Kolorenc and L. Mitás, *Phys. Rev. Lett.* **101**, 185502 (2008).
- ¹⁸ D. Alfe, M. J. Gillan, M. D. Towler, and R. J. Needs, *Phys. Rev. B* **70**, 214102 (2004), ISSN 1098-0121.
- ¹⁹ P. J. Reynolds, D. M. Ceperley, B. J. Alder, and W. A. Lester, *J. Chem. Phys.* **77**, 5593 (1982).
- ²⁰ Wirawan Purwanto, Henry Krakauer, and Shiwei Zhang, *Phys. Rev. B* **80**, 214116 (2009), ISSN 1098-0121.
- ²¹ S. Zhang and H. Krakauer, *Phys. Rev. Lett.* **90**, 136401 (2003).
- ²² C. J. Umrigar, J. Toulouse, C. Filippi, S. Sorella, and R. G. Hennig, *Phys. Rev. Lett.* **98**, 110201 (2006).
- ²³ Hendra Kwee, Shiwei Zhang, and Henry Krakauer, *Phys. Rev. Lett.* **100**, 126404 (2008), ISSN 0031-9007.
- ²⁴ T. D. Beaudet, M. Casula, J. Kim, S. Sorella, and R. M. Martin, *J. Chem. Phys.* **129**, 164711 (2008).
- ²⁵ M. Casula, C. Attaccalite, and S. Sorella, *J. Chem. Phys.* **121**, 7110 (2004).
- ²⁶ P. Giannozzi et al., *J. Phys.: Condens. Matter* **21**, 395502 (2009).
- ²⁷ K. Schwarzland and P. Blaha, *Comput. Mater. Sci.* **28**, 259 (2003).
- ²⁸ F. Gygi, *Qbox* (2010), URL <http://eslab.ucdavis.edu/software/qbox/>.
- ²⁹ S. Sorella, *Turborvb* (2010), URL <http://turborvb.qe-forge.org/>.
- ³⁰ M. Casula, C. Filippi, and S. Sorella, *Phys. Rev. Lett.* **95**, 100201 (2005).
- ³¹ J. R. Trail and R. J. Needs, *The Journal of Chemical Physics* **122**, 174109 (pages 10) (2005), URL <http://link.aip.org/link/?JCP/122/174109/1>.
- ³² M. Burkatzki, C. Filippi, and M. Dolg, *Jour. Chem. Phys.* **126**, 234105 (2007).
- ³³ N. Troullier and J. L. Martins, *Phys. Rev. B* **43**, 1993 (1991).
- ³⁴ M. Casula and S. Sorella, *J. Chem. Phys.* **119**, 6500 (2003).
- ³⁵ C. J. Umrigar, J. Toulouse, C. Filippi, S. Sorella, and R. G. Hennig, *Phys. Rev. Lett.* **98**, 110201 (2006).
- ³⁶ Manuela Capello, Federico Becca, Michele Fabrizio, and Sandro Sorella, *Phys. Rev. B* **77**, 144517 (2008).
- ³⁷ S. Azadi, C. Cavazzoni, and Sandro Sorella, *Phys. Rev. B* **82**, 125112 (2010).
- ³⁸ T. H. Dunning Jr., *J. Chem. Phys.* **90**, 1007 (1989).
- ³⁹ K. A. Peterson and T. H. Dunning Jr., *J. Chem. Phys.* **117**, 10548 (2002).
- ⁴⁰ M. Casula, S. Moroni, S. Sorella, and C. Filippi, *J. of Chem. Phys.* **132**, 154113 (2010).
- ⁴¹ P. E. Blöchl, *Phys. Rev. B* **50**, 17953 (1994).
- ⁴² G. Kresse and D. Joubert, *Phys. Rev. B* **59**, 1758 (1999).
- ⁴³ M. Methfessel and A. T. Paxton, *Phys. Rev. B* **40**, 3616 (1989).
- ⁴⁴ V. V. Brazhkin, A. G. Lyapin, S. V. Popova, and R. N. Voloshin, *Phys. Rev. B* **51**, 7549 (1995).
- ⁴⁵ L. Kleinman and D. M. Bylander, *Phys. Rev. Lett.* **48**, 1425 (1982).
- ⁴⁶ P. L. Blöchl, *Phys. Rev. B* **41**, 5414 (1990).
- ⁴⁷ S. Fahy, X. W. Wang, and Steven G. Louie, *Phys. Rev. B* **42**, 3503 (1990).
- ⁴⁸ L. Mitáš, E. L. Shirley, and D. M. Ceperley, *J. Chem. Phys.* **95**, 3467 (1991).
- ⁴⁹ C. J. Umrigar, private communication (2010).
- ⁵⁰ J. P. Perdew and A. Zunger, *Phys. Rev. B* **23**, 5048 (1981).
- ⁵¹ M. Hill, ed., *Properties of Crystalline Silicon* (INSPEC, London, 1999).
- ⁵² M.T. Yin and M.L. Cohen, *Phys. Rev. B* **26**, 5668 (1982).
- ⁵³ K. P. Esler, R. E. Cohen, B. Militzer, Jeongnim Kim, R. J. Needs, and M. D. Towler, *Phys. Rev. Lett.* **104**, 185702 (2010).
- ⁵⁴ M. Casula, *Phys. Rev. B* **74**, 161102 (2006).
- ⁵⁵ G. B. Bachelet, D. M. Ceperley, and M. G. B. Chiochetti, *Phys. Rev. Lett.* **62**, 2088 (1989), ISSN 0031-9007.
- ⁵⁶ The pseudopotentials not available in the semilocal Gaussian form, as those generated by the atomic PWSCF code, have been fitted by a series of Gaussian functions. The discrepancy in the transition pressure obtained by the fitted pseudopotentials is less than 0.15 GPa from the original one.
- ⁵⁷ It is clear that with the PBC+APBC average of the KZK corrected energies we can reduce the error on the final transition pressure well below the 20 meV/atom threshold reached in Ref. 13.
- ⁵⁸ The parameters of the PAW data set are $r_s = 2.1$, $r_p = 2.1$, $r_d = 2.0$ (d is local). The nonlocal channels are fitted at the eigenvalue and at 6.0 Ry for s and p . The unbound d channel is at $\epsilon = -0.3$ Ry.
- ⁵⁹ Early attempts to generate PP's at the QMC level was done in Ref. 55